Complete Assignment of the Hydrogen Out-of-Plane Wagging Vibrations of Bathorhodopsin: Chromophore Structure and Energy Storage in the Primary Photoproduct of Vision†

Ilona Palings,‡ Ellen M. M. van den Berg,§ Johan Lugtenburg,§ and Richard A. Mathies*,‡

Department of Chemistry, University of California, Berkeley, California 94720, and Department of Chemistry, University of Leiden, 2300 RA Leiden, The Netherlands

Received July 12, 1988; Revised Manuscript Received September 23, 1988

ABSTRACT: Resonance Raman vibrational spectra of the retinal chromophore in bathorhodopsin have been obtained after regenerating bovine visual pigments with an extensive series of ^{13}C- and deuterium-labeled retinals. A low-temperature spinning cell technique was used to produce high-quality bathorhodopsin spectra exhibiting resolved hydrogen out-of-plane wagging vibrations at 838, 850, 858, 875, and 921 cm^{-1}. The isotopic shifts and a normal coordinate analysis permit the assignment of these lines to the $HC_7{=}C_8H$ B_g, $C_{14}H$, $C_{12}H$, $C_{10}H$, and $C_{11}H$ hydrogen out-of-plane wagging modes, respectively. The coupling constant between the $C_{11}H$ and $C_{12}H$ wags as well as the $C_{12}H$ wag force constant are unusually low compared to those of retinal model compounds. This quantitatively confirms the lack of coupling between the $C_{11}H$ and $C_{12}H$ wags and the low $C_{12}H$ wag vibrational frequency noted earlier by Eyring et al. [(1982) *Biochemistry 21*, 384]. The force constants for the $C_{10}H$ and $C_{14}H$ wags are also significantly below the values observed in model compounds. We suggest that the perturbed hydrogen out-of-plane wagging and C–C stretching force constants for the $C_{10}{-}C_{11}{=}C_{12}{-}C_{13}$ region of the chromophore in bathorhodopsin result from electrostatic interactions with a charged protein residue. This interaction may also contribute to the 33 kcal/mol energy storage in bathorhodopsin.

Visual excitation begins with the 11-cis to 11-trans photoisomerization of the retinal chromophore (I) in the visual

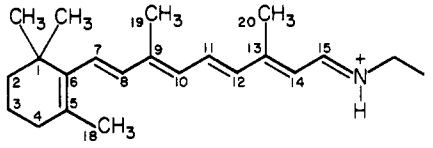

I

pigment rhodopsin (Yoshizawa & Wald, 1963; Birge, 1981). Rhodopsin is converted to its primary photoproduct, bathorhodopsin, in <6 ps (Peters et al., 1977), and 33 kcal/mol is stored in this transition (Cooper, 1979; Schick et al., 1987). The mechanism of this rapid isomerization and of the energy storage has been examined in great detail (Honig et al., 1979b; Warshel & Barboy, 1982; Birge & Hubbard, 1980, 1981; Birge et al., 1988; Loppnow & Mathies, 1988). However, a complete molecular interpretation has not yet emerged.

Structural information about the chromophore in the primary photoproduct can be obtained with resonance Raman spectroscopy. Intense vibrational lines at 854, 876, and 922 cm^{-1} in the resonance Raman spectrum of bathorhodopsin (Figure 1) provide a unique signature of the chromophore structure (Oseroff & Callender, 1974; Eyring & Mathies, 1979). Eyring et al. (1980a,b, 1982) assigned these lines to hydrogen out-of-plane (HOOP)[1] wagging vibrations of the chromophore on the basis of their shifts in bathorhodopsin derivatives containing deuteriated chromophores. It was noted that the unusual $C_{11}H$ wag frequency (922 cm^{-1}) and the lack of coupling between the $C_{11}H$ wag and the $C_{12}H$ wag were due in part to the low $C_{12}H$ wag frequency. Eyring et al. (1982) proposed that the frequency perturbations were induced by a charged binding site residue, possibly the same residue that is responsible for the opsin shift in rhodopsin (Arnaboldi et al., 1979).

In previous resonance Raman experiments, bathorhodopsin was trapped in a photostationary steady state at 77 K along with rhodopsin (~30%) and isorhodopsin (~20%). With this technique one can obtain a pure bathorhodopsin spectrum only via subtraction of the contributions of rhodopsin and isorhodopsin (Eyring & Mathies, 1979; Aton et al., 1980). To resolve this problem, a low-temperature spinning cell technique has been developed, with which nearly pure bathorhodopsin spectra can be obtained directly (Palings et al., 1987). The signal-to-noise ratio in these spectra is very good since fluorescence backgrounds are diminished, and higher resolution is obtained because line-broadening effects due to sample heating are avoided. An extensive set of deuterium and ^{13}C derivatives permit the complete assignment of the HOOP modes in the 835–920-cm^{-1} region. A normal mode analysis is performed to evaluate these assignments and to obtain normal mode descriptions and force constants. This analysis quantitatively confirms the earlier conclusions of Eyring et al. (1980b, 1982) that the $C_{11}{=}C_{12}$ region of the bathorhodopsin chromophore is strongly perturbed by the protein. These perturbations may contribute to the 33 kcal/mol energy storage in the primary photoproduct (Cooper, 1979; Schick et al., 1987).

† This research was supported by the National Institutes of Health (EY-02051), the Netherlands Foundation for Chemical Research (SON), and the Netherlands Organization for the Advancement of Pure Research (NWO).

* Correspondence should be addressed to this author.

‡ University of California.

§ University of Leiden.

[1] Abbreviations: HOOP, hydrogen out of plane; PSB, protonated Schiff base.

0006-2960/89/0428-1498$01.50/0

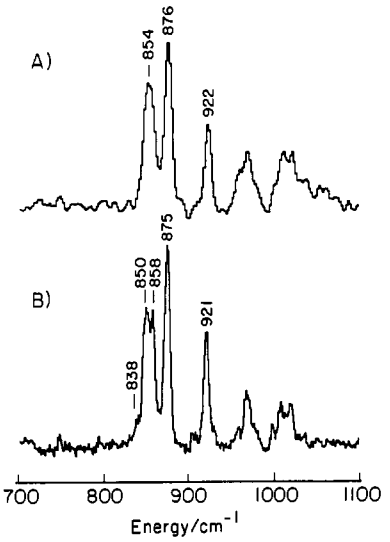

FIGURE 1: Comparison of 77 K bathorhodopsin spectra obtained with a stationary sample (A) and with a spinning sample (B).

Materials and Methods

Retinal Synthesis. The syntheses and characterization of the isotopically labeled retinal derivatives have been described by Lugtenburg and co-workers [Fransen et al., 1980 (18-D_3; 19-D_3); Broek & Lugtenburg, 1980 (10-D; 11-D; 12-D; 11,12-D_2); Broek & Lugtenburg, 1982 (10-D; 11-D; 10,11-D_2; 14,20-D_4); Pardoen et al., 1983 (10-^{13}C; 11-^{13}C; 19-^{13}C; 20-^{13}C); Pardoen et al., 1984 (14-D; 14-^{13}C; 15-^{13}C; 14,15-di-^{13}C; 14,15-D_2; 14-^{13}C,15-D; 15-^{13}C,15-D; 14,15-di-^{13}C,15-D); Pardoen et al., 1985 (8-^{13}C; 9-^{13}C; 12-^{13}C; 13-^{13}C; Pardoen et al., 1986 (20-D_3; 12,20-D_4; 12,14,20-D_5; 11,14-D_2; 12,14-D_2; 12,14-D_2,20-^{13}C); Courtin et al., 1985 (5-^{13}C; 6-^{13}C; 7-^{13}C; 18-^{13}C)]. Reviews of these synthetic procedures have been presented by Lugtenburg (1984, 1985) and by Lugtenburg et al. (1988).

Rhodopsin Preparation. Rod outer segments were isolated from bovine retinas as described by Palings et al. (1987). The yield was typically 15 nmol of rhodopsin/retina. The isolated rod outer segments were lysed in water, suspended in phosphate buffer which contained hydroxylamine (~200-fold excess), and bleached in ambient light. Excess hydroxylamine was removed by washing with phosphate buffer. Pigments were regenerated in phosphate buffer at room temperature with the appropriate isotopically labeled 9-*cis*- or 11-*cis*-retinals. The regenerated pigments were solubilized in Ammonyx-LO and purified by hydroxylapatite chromatography (Applebury et al., 1974). The purified pigment was concentrated with Amicon Centriflo CF25 membrane cones to approximately 0.5 mL (40 OD/cm at 500 nm). Deuteriated samples were obtained by washing the concentrated pigment solution twice with D_2O buffer.

Raman Experiments. Spectra were obtained by using the spinning cell technique devised by Braiman and Mathies (1982). The rhodopsin or isorhodopsin sample was frozen at 77 K in a circular groove in a conical copper tip. The rotating, frozen sample was irradiated on one side of the tip with an unfocused 476.2-nm pump beam (~150 mW) which creates a photostationary steady-state mixture containing approximately 25% rhodopsin, 60% bathorhodopsin, and 15% isorhodopsin (Oseroff & Callender, 1974; Eyring & Mathies, 1979; Aton et al., 1980). The other side of the tip was excited with a 568.2-nm probe beam (5–10 mW, focused with a 60-mm focal length lens) which selectively enhances the scattering from bathorhodopsin. The Raman scattering was detected with a photon-counting double-monochromator system. Spectral slit widths were 2 cm^{-1}. The spectra were corrected for the sensitivity of the detection system, and fluorescence backgrounds were subtracted by using a quartic background fitting algorithm. Frequencies are accurate to 1 cm^{-1} and were determined by Lorentzian band deconvolution.

Table I: Out-of-Plane Valence Force Field for Bathorhodopsin

force constant[b]	initial[a]	refined	force constant[b]	initial[a]	refined
T (C=C)	0.545	0.490	WW (5R, 6R)	0.172	0.172
T (C=N)	0.545[c]	0.560	WW (6R, 7H)	0.0	0.0
T (C–C)	0.197	0.197	WW (7H, 8H)	0.172	0.172
T (N–C)	0.081[c]	0.081	WW (10H, 11H)	0.061	0.043
T (C–Me)	0.081	0.081	WW (11H, 12H)	0.168	0.132
W (C–Me)	0.57	0.57	WW (14H, 15H)	0.055	0.060
W (7H)	0.476	0.482	WW (15H, NH)	0.138[c]	0.164
W (8H)	0.482	0.480	WW (8H, 9Me)	0.068	0.031
W (10H)	0.466	0.425	WW (12H, 13Me)	0.055	0.031
W (11H)	0.472	0.463	WW (9Me, 10H)	0.174	0.127
W (12H)	0.469	0.415	WW (13Me, 14H)	0.172	0.127
W (14H)	0.453	0.420	WW (10H, 12H)	0.0	−0.021
W (15H)	0.448	0.550	WW (8H, 10H)	0.0	−0.016
W (NH)	0.386[c]	0.400	WW (12H, 14H)	0.0	−0.026
TH (CC, CCH)	0.056	0.056	WW (14H, NH)	0.0	−0.005
			TW (C=C, CMe)	0.292	0.262
TH (CN, NCH)	0.056	0.056	TW (C–C, CMe)	−0.116	−0.116
			TW (CMe, CMe)	−0.052	−0.052
WH (CMe, CCH)	0.08	0.08			
WH (CH, CCH)	0.018	0.018			
WH (CH, NCH)	0.018	0.027			

[a] These force constants were transferred from the analysis of *all-trans*-retinal (Curry et al., 1982, 1984; Curry, 1983). [b] Coordinate definitions are H, valence bend; T, torsion; and W, out-of-plane wag. All internal coordinates except for the methyl torsion are defined following Wilson et al. (1955). The methyl torsion is defined as a rigid rotation of the methyl group. Wags are defined positive if the wagging atom moves in the $+Z$ direction. Units are mdyn·Å/rad^2 for WW, TT, TW, HT, and HW interactions. The complete force field for bathorhodopsin can be found in Palings (1987). [c] These force constants were transferred from the analysis of the protonated Schiff base chromophore in BR_{568} (Smith et al., 1987a).

Figure 1 compares bathorhodopsin spectra obtained with the stationary sample and spinning cell techniques. With a spinning sample, the signal-to-noise ratio is improved and line-broadening effects due to sample heating are eliminated. Another advantage of the spinning cell is the elimination of fluorescence created by the pump beam. This allows reduction of the probe laser power to such a low level that the photoconversion of bathorhodopsin back to rhodopsin and isorhodopsin by the probe beam is minimized, thereby enhancing the contribution of bathorhodopsin scattering to the raw data.

Normal Mode Calculations. The *all-trans*-retinal protonated Schiff base chromophore was simplified by replacing atoms 1, 4, and 18 with R groups, where R is an atom having mass 15, unit valence, and the parameters of a saturated carbon atom. The lysine was replaced by a CH_2R group. The out-of-plane force field developed for *all-trans*-retinal (Curry et al., 1982; Curry, 1983) was used as the starting point (Table I). Force constants were added for the C=N and N–C torsions, the NH wag, and the interaction constant between the $C_{15}H$ and NH wags (15H × NH). These lysine force constants are similar to those employed in the vibrational analysis of BR_{568} (Smith et al., 1987a). The force field was refined by adjusting 20 force constants to fit 66 frequencies observed in the deuterium derivatives. These included the 7H, 8H, 10H, 11H, 12H, 14H, and 15H wag diagonal force constants and the off-diagonal coupling constants between adjacent wagging coordinates (7H × 8H, 8H × 9Me, 9Me

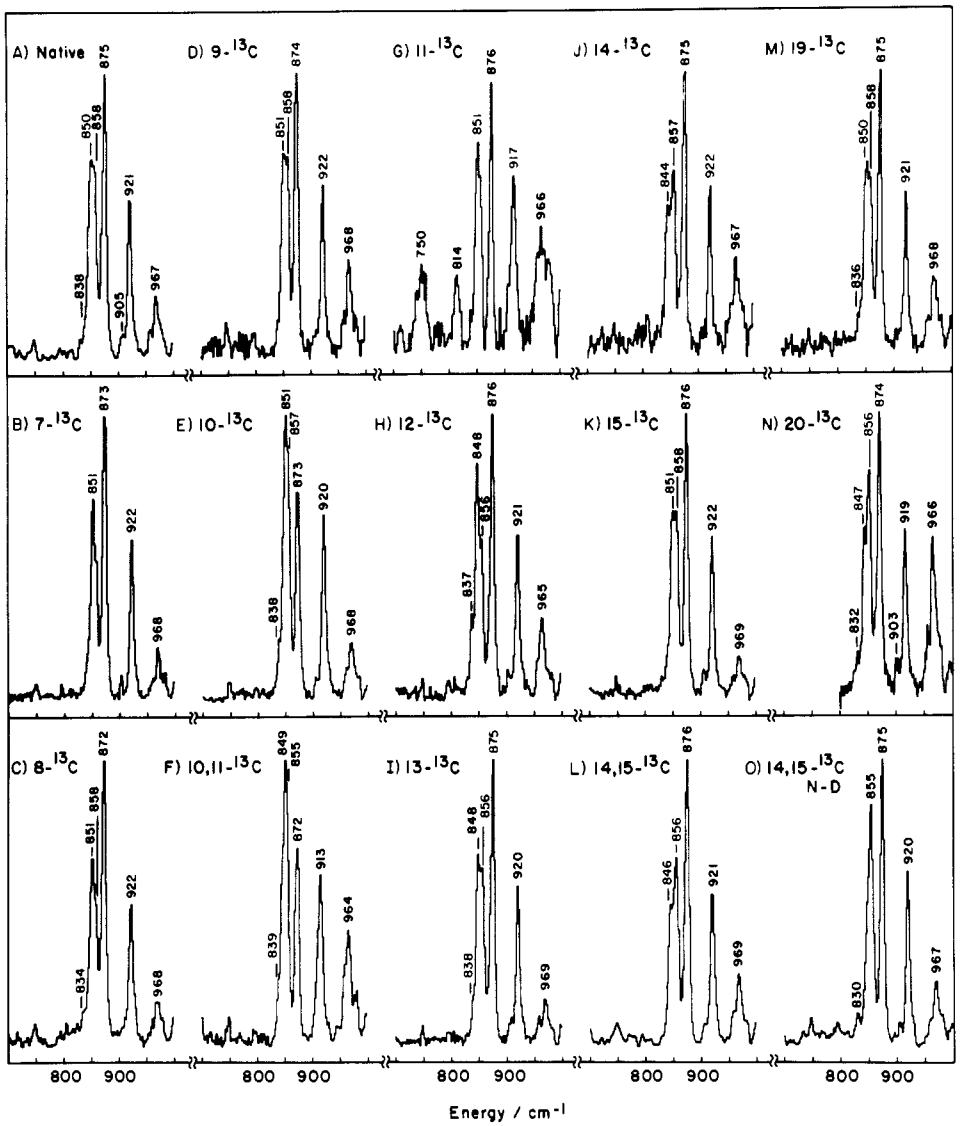

FIGURE 2: Resonance Raman spectra of (A) unmodified, (B) 7-^{13}C, (C) 8-^{13}C, (D) 9-^{13}C, (E) 10-^{13}C, (F) 10,11-^{13}C, (G) 11-^{13}C, (H) 12-^{13}C, (I) 13-^{13}C, (J) 14-^{13}C, (K) 15-^{13}C, (L) 14,15-^{13}C, (M) 19-^{13}C, (N) 20-^{13}C, and (O) 14,15-^{13}C,*N*-D bathorhodopsin.

× 10H, 10H × 11H, 11H × 12H, 12H × 13Me, 13Me × 14H, and 14H × 15H). The 8H × 9 Me and 12H × 13 Me interaction constants were constrained to be equal, as well as the 9Me × 10H and 13Me × 14H interaction constants. In the course of the refinement it was necessary to add 8H × 10H, 10H × 12H, 12H × 14H, and 14H × NH interaction constants to fit to the data. These 1–3 interactions were not included in our previous calculations on retinals because they are expected to be small and the previous data sets were not sufficiently extensive to constrain these coupling constants. However, if these interaction constants were not included in the bathorhodopsin calculations, the HOOP modes split apart too much due to coupling between wags three carbon atoms apart. After refinement the average error in the 66 calculated frequencies was ±2.1 cm^{-1}.

The intensity of the wagging vibrations in the resonance Raman spectra argues that the chromophore in bathorhodopsin has a distorted geometry (Eyring et al., 1980a; Warshel & Barboy, 1982). Our calculations were performed on a chromophore that was twisted in the same direction about the C_8–C_9, C_{10}–C_{11}, C_{12}–C_{13}, and C_{14}–C_{15} single bonds by 20° [see Eyring et al. (1982) and Warshel and Barboy (1982)]. This geometric distortion introduces small changes in the kinetic constants which produce <4-cm^{-1} shifts in the HOOP modes. Since this molecule is not planar, separation of the normal modes into in-plane and out-of-plane symmetry groups is not rigorously valid, and kinetic and potential interactions between in-plane and out-of-plane coordinates should be included. To investigate the importance of these interactions, QCFF-PI calculations were performed on the flat and the twisted chromophore geometry. Frequency shifts of 10–15 cm^{-1} were observed upon twisting, and the normal mode coefficients were very similar. This suggests that the addition of kinetic and potential interactions between in-plane and out-of-plane coordinates will not greatly affect our results. Therefore, to reduce computation time, these interactions were omitted.

Results

Figures 2–4 present spectra of the bathorhodopsin isotopic derivatives. The crosshatching indicates lines that are due to rhodopsin and isorhodopsin. They were identified by comparison of the 77 K steady-state spectra with spectra of the pure rhodopsin and isorhodopsin derivatives and by correlating pump beam induced changes in the line intensities with the expected changes in bathorhodopsin concentrations. Lorentzian deconvolution of the bands in the 800–950-cm^{-1} region results in the normal mode frequencies presented in Table II. In unmodified bathorhodopsin, five hydrogen out-of-plane wagging vibrations can be identified at 921, 875, 858, 850, and 838 cm^{-1}. The empirical assignments of the hydrogen

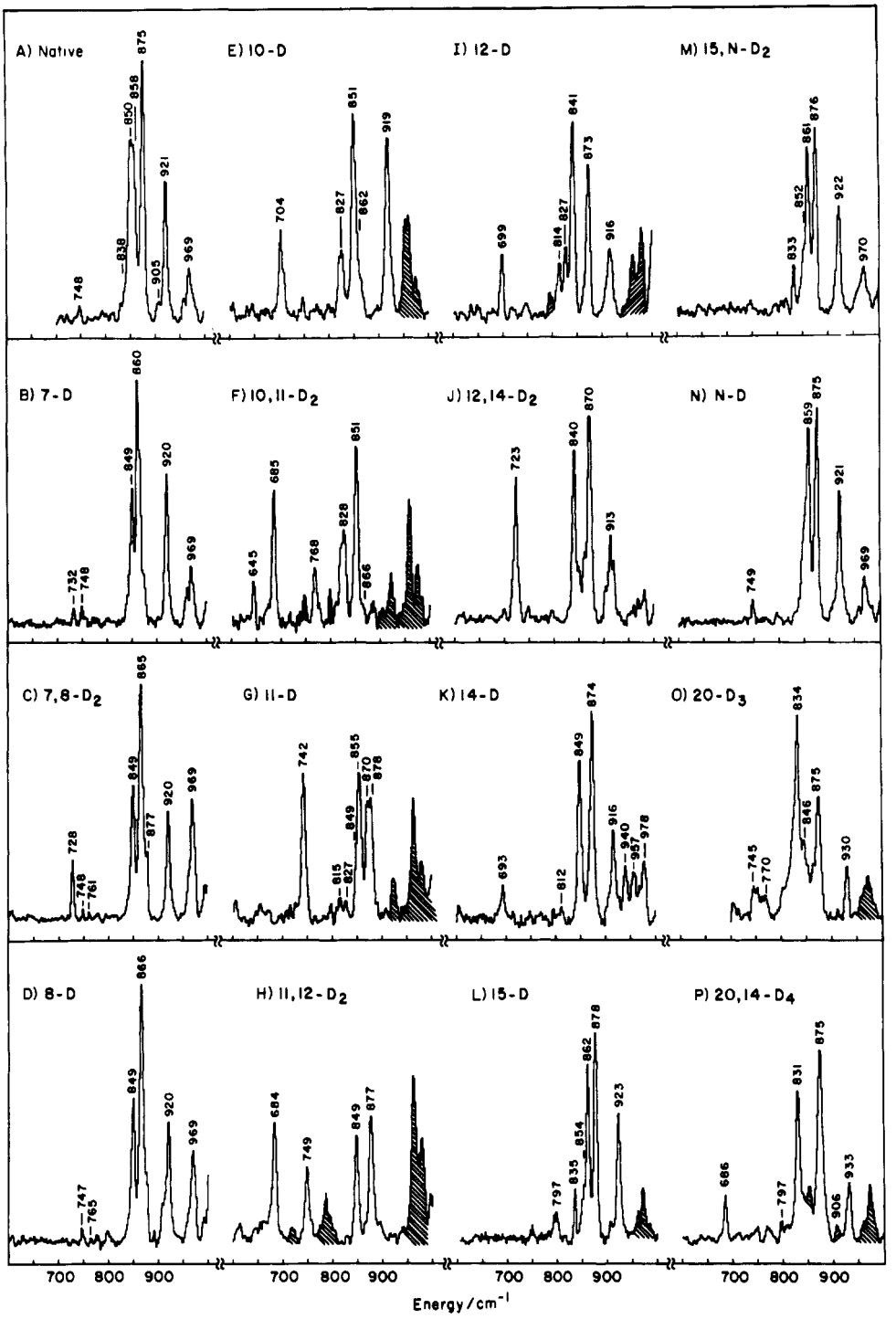

FIGURE 3: Resonance Raman spectra of (A) unmodified, (B) 7-D, (C) 7,8-D_2, (D) 8-D, (E) 10-D, (F) 10,11-D_2, (G) 11-D, (H) 11,12-D_2, (I) 12-D, (J) 12,14-D_2, (K) 14-D, (L) 15-D, (M) 15,N-D_2, (N) *N*-D, (O) 20-D_3, and (P) 20,14-D_4 bathorhodopsin. The spectra of 10-D, 10,11-D_2, 11-D, 11,12-D_2, 12-D, 15-D, 15,N-D_2, and 20,14-D_4 bathorhodopsin were taken from Eyring et al. (1980b, 1982).

out-of-plane lines will be discussed below and compared with the results of the normal mode calculation which are also summarized in Table II. The observed and calculated ^{13}C- and deuterium-induced shifts of the HOOP modes in selected derivatives are summarized in Figures 5 and 6.

Before examining the HOOP modes of bathorhodopsin in detail it is useful to know that the HOOP modes in linear polyenes are made up primarily of linear combinations of the wag coordinates (Curry et al., 1982, 1985). In retinal protonated Schiff bases, the presence of the methyl groups at C_9 and C_{13} subdivides the chain HOOP modes into three vibrationally isolated groups: the C_7 and C_8 hydrogens, the C_{10}, C_{11}, and C_{12} hydrogens, and the C_{14}, C_{15}, and N hydrogens. Within these groups, the wags couple strongly across the double bonds and weakly across the single bonds. Thus, the C_7H and C_8H, the $C_{11}H$ and $C_{12}H$, and the $C_{15}H$ and NH wag coordinates couple strongly, forming in-phase and out-of-phase normal modes at ~960 cm^{-1} (A_u) and ~830 cm^{-1} (B_g), respectively. The $C_{10}H$ and $C_{14}H$ wag coordinates are observed as isolated modes at lower frequency (~880 cm^{-1}).

The 921-cm^{-1} Mode. This line was previously assigned to the $C_{11}H$ wag by Eyring et al. (1982) on the basis of its disappearance in 11-D and 11,12-D_2 bathorhodopsin (Figure 3G,H). In 11-D bathorhodopsin it shifts to 742 cm^{-1}; the intensity remaining at 922 cm^{-1} is due to scattering from rhodopsin and isorhodopsin (Eyring et al., 1982). In 12-D

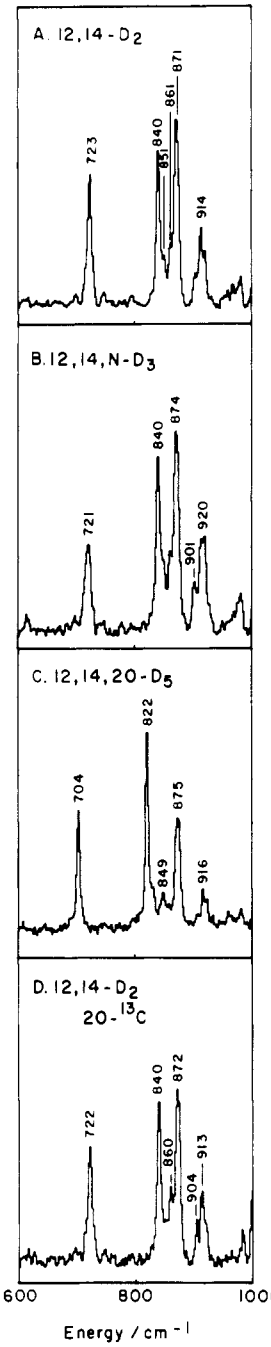

FIGURE 4: Resonance Raman spectra of (A) 12,14-D_2, (B) 12,14,*N*-D_3, (C) 12,14,20-D_5, and (D) 12,14-D_2,20-^{13}C bathorhodopsin.

bathorhodopsin, this mode shifts down only 5 cm^{-1} to 916 cm^{-1}, indicating that the $C_{11}H$ and $C_{12}H$ wag coordinates are virtually uncoupled. Our ^{13}C data provide additional support for this assignment. The isotopic shift for the 921-cm^{-1} mode is largest (4 cm^{-1}) in the 11-^{13}C derivative (Figure 5). The 921-cm^{-1} mode, therefore, contains predominantly the $C_{11}H$ wag coordinate. The absence of a shift of the 921-cm^{-1} mode in 12-^{13}C bathorhodopsin confirms that the $C_{12}H$ wag coordinate does not contribute to the 921-cm^{-1} mode.

The normal mode calculation predicts that the 921-cm^{-1} mode consists of the $C_{11}H$ wag coordinate (coefficient 0.97) mixed somewhat with the $C_{12}H$ and $C_{10}H$ wags (Table II). The calculation accurately reproduces the frequency of the $C_{11}H(D)$ mode in the native, 11-D, 10,11-D_2, and 11,12-D_2 molecules (Figure 6). In 12-D bathorhodopsin the predicted frequency drop is 11 cm^{-1} (922 → 911 cm^{-1}) while the observed drop is 5 cm^{-1}. This indicates that the calculation

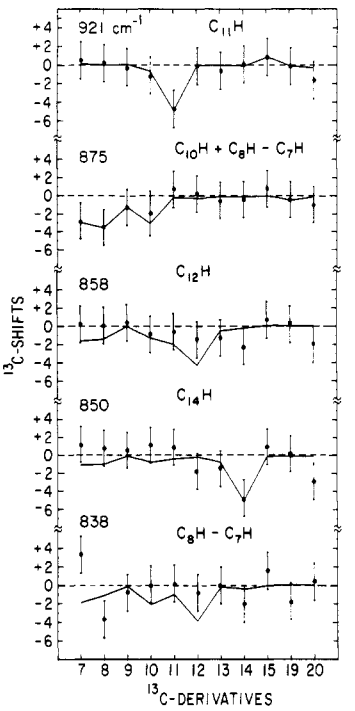

FIGURE 5: Observed and calculated (—) ^{13}C shifts of the HOOP modes in bathorhodopsin.

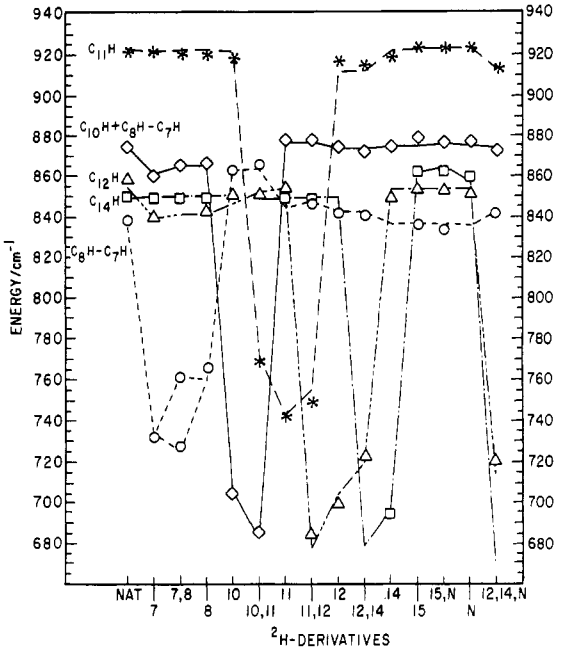

FIGURE 6: Observed (points) and calculated (lines) frequencies for the HOOP modes in the deuterium derivatives of bathorhodopsin.

predicts too much coupling between the $C_{11}H$ and $C_{12}H$ wag coordinates. Comparison of the calculated and observed ^{13}C shifts (Figure 5) provides an empirical check on the calculated normal mode coefficients, since ^{13}C substitution results in only a small perturbation of the normal mode character. The calculation correctly reproduces the ^{13}C shifts for this mode in the 10-, 11-, and 12-^{13}C derivatives.

The 875-cm^{-1} Mode. This line was assigned to the $C_{10}H$ wag by Eyring et al. (1982) on the basis of its shift to 704 cm^{-1} in 10-D and to 685 cm^{-1} in 10,11-D_2 bathorhodopsin (Figure 3E,F). Our new data show that the 875-cm^{-1} line is also sensitive to isotopic substitution at C_7 and C_8: it shifts to 860 cm^{-1} in 7-D, to 866 cm^{-1} in 8-D, to 873 cm^{-1} in 7-^{13}C, and to 872 cm^{-1} in 8-^{13}C bathorhodopsin. This indicates that the

875-cm^{-1} mode also contains C_7H and C_8H wag character.

The calculation predicts that the 875-cm^{-1} mode is a combination of the $C_{10}H$, C_7H, and C_8H wag coordinates (Table II). The $C_{10}H$ wag (coefficient 0.74) is mixed almost equally with the out-of-phase (B_g) combination of the C_7H wag (0.70) and the C_8H wag (0.55). Figure 6 shows that the calculation accurately predicts the frequency of this mode in the deuterium derivatives. In particular, its shift in the 7D, 8D, and 7,8-D_2 derivatives is reproduced, indicating that the interaction of the $C_{10}H$ wag with the $HC_7{=}C_8H$ B_g wag combination is correct. Figure 5 shows that the normal mode calculation also predicts the ^{13}C shifts of the 875-cm^{-1} mode accurately.

The 850-cm^{-1} Mode. Eyring et al. (1982) observed three bathorhodopsin lines in the 800–950-cm^{-1} region: the 921- and 875-cm^{-1} lines, which we have discussed above, and a broad band at ~854 cm^{-1}. They tentatively assigned this band to the $C_{14}H$ wag. The $C_{12}H$ wag was thought to lie in the 830–860-cm^{-1} region but could not be explicitly identified. With the increased resolution of the spinning cell technique and Lorentzian band deconvolution, we have resolved the 854-cm^{-1} band into three lines, at 858, 850, and 838 cm^{-1}. The fact that the deuteriated wag modes in the 12-D, 14-D, and 7,8-D_2 derivatives all have intensity suggests that all three coordinates contribute intensity to lines in the 800–860-cm^{-1} region. Hence, the 858-, 850-, and 838-cm^{-1} lines must be assigned to some combination of the $C_{12}H$, $C_{14}H$, and $HC_7{=}C_8H$ B_g wag coordinates.

We assign the 850-cm^{-1} line as a localized $C_{14}H$ wag. The 850-cm^{-1} line is most sensitive to ^{13}C substitution at C_{14}, which causes a 6-cm^{-1} shift (Figure 5). In the 14,15-di-^{13}C derivative (Figure 2L) it also shifts significantly (4 cm^{-1}), but in the 15-^{13}C derivative no shift is observed. These data indicate that the 850-cm^{-1} mode contains predominantly the $C_{14}H$ wag coordinate. This assignment is consistent with the shifts observed in the deuterium derivatives. In the 14-D derivative, the $C_{14}D$ wag appears at 693 cm^{-1} and the 858- and 850-cm^{-1} doublet collapses to one line at 849 cm^{-1}, which is assigned as the down-shifted $C_{12}H$ HOOP mode. The shift of the 850-cm^{-1} mode in response to 15-D and *N*-D substitution (Figure 3L,N) also supports our assignment. In the 15-D derivative, the 850-cm^{-1} line shifts up to 862 cm^{-1}, and in the *N*-D derivative it shifts to 859 cm^{-1}. These upshifts are due to coupling of the $C_{14}H$ wag coordinate with the $C_{15}D$ (or ND) wags (see below).

The 850-cm^{-1} mode is calculated as predominantly the $C_{14}H$ wag (coefficient 0.90). Figure 6 compares the calculated and observed frequencies for this mode in the deuteriated derivatives. The $C_{14}D$ wag in 14-D bathorhodopsin is calculated at 696 cm^{-1} (observed at 693 cm^{-1}). In 12,14-D_2 and 12,14,*N*-D_3 bathorhodopsin, the symmetric combination of the $C_{12}D$ and $C_{14}D$ wags is calculated at 720 cm^{-1} (observed 723 cm^{-1}) and 713 cm^{-1} (observed 721 cm^{-1}), respectively. The 12D × 14D × ND interaction may not be modeled correctly, since we do not know the frequencies of the NH or ND wag modes. However, the calculation does satisfactorily predict the upshift of the $C_{14}H$ mode in 15-D, *N*-D, and 15,*N*-D_2 bathorhodopsin. Finally, Figure 5 shows that the normal mode calculation predicts the ^{13}C shifts for the 850-cm^{-1} mode reasonably well. The calculation is unable to reproduce the shift observed with substitution at C_{20}, but this may be complicated by shifts of underlying methyl stretching modes which were not included in the calculation.

The 858- and 838-cm^{-1} Modes. The two lines at 858 and 838 cm^{-1} can be assigned to the $C_{12}H$ and $HC_7{=}C_8H$ B_g modes. If C_{12} and C_{14} are both deuteriated, the line left behind in the 830–860-cm^{-1} region must be assigned as the $HC_7{=}C_8H$ B_g HOOP. In the spectrum of 12,14-D_2 bathorhodopsin (Figure 3J), the 840-cm^{-1} line is quite prominent and is assigned as the $HC_7{=}C_8H$ B_g mode. Assignment of this line to the $HC_7{=}C_8H$ B_g HOOP seemed at first inconsistent with its sensitivity to deuteriation at C_{20} (in 12,14,20-D_5 bathorhodopsin it appears to shift to 822 cm^{-1}). This observation suggested that the 840-cm^{-1} mode in the 12,14-D_2 derivative might be due to the C_{13}–Me stretch.[2] This hypothesis was tested with the 12,14-D_2,20-^{13}C derivative (Figure 4D). Since no shift of the 840-cm^{-1} line is observed, we abandoned the C_{13}–Me assignment. The hypothesis that the 840-cm^{-1} line in 12,14-D_2 bathorhodopsin is due to the NH wag was tested with the 12,14,*N*-D_3 derivative (Figure 4B). Since the 840-cm^{-1} mode did not shift upon N-deuteriation, we also abandoned this assignment.[3] Therefore, the 840-cm^{-1} line in 12,14-D_2 bathorhodopsin is assigned to the $HC_7{=}C_8H$ B_g HOOP, and the 838-cm^{-1} line in unmodified bathorhodopsin is also assigned to the $HC_7{=}C_8H$ B_g HOOP. Unfortunately, the ^{13}C shifts summarized in Figure 5 do not provide any obvious confirmation or denial of our analysis. The reliability of the ^{13}C shifts for the 838-cm^{-1} mode is uncertain because it is such a weak shoulder.

The calculation predicts that the 838-cm^{-1} mode is the $HC_7{=}C_8H$ B_g wag combination mixed strongly with the $C_{10}H$ and $C_{12}H$ wags. The calculation does a good job of reproducing the deuteriated wag frequencies in the 7D, 8D, and 7,8-D_2 derivatives (Figure 6). Since the $C_{10}H$ wag and the $HC_7{=}C_8H$ B_g wag combination are coupled, one expects the 838-cm^{-1} mode to shift up when C_{10} is deuteriated. In 10-D bathorhodopsin the 838-cm^{-1} line disappears and a new shoulder appears at 862 cm^{-1} (Figure 3E). The calculation predicts that the new line at 862 cm^{-1} is due to the upshifted $HC_7{=}C_8H$ B_g mode. The calculated coefficients suggest that the increased intensity of the 840-cm^{-1} line in the 12,14-D_2 spectrum compared to the native spectrum is due to the increased contribution of the $C_{10}H$ wag.

The $C_{12}H$ wag is assigned at 858 cm^{-1}. ^{13}C substitution at C_{12} causes the lines at 858 and 850 cm^{-1} to shift 2 cm^{-1}. This shows that there is significant $C_{12}H$ wag character in both the 850- and 858-cm^{-1} modes. The 858-cm^{-1} line shifts when ^{13}C is placed at positions 13 and 14, indicating that it also contains $C_{14}H$ wag character. In 12-D bathorhodopsin, the $C_{12}D$ wag is seen at 699 cm^{-1} and no modes are observed in the 850–858-cm^{-1} region, again indicating that the $C_{12}H$ wag lies in the 858-cm^{-1} band. The 841-cm^{-1} line in the 12-D spectrum is assigned as the antisymmetric combination of the $C_{10}H$ with the $HC_7{=}C_8H$ B_g. The $C_{14}H$ wag apparently loses intensity and is not observed.

The 858-cm^{-1} mode is calculated as predominantly $C_{12}H$ wag (coefficient +0.88) mixed with the antisymmetric combination of the $C_{10}H$ wag and the $HC_7{=}C_8H$ B_g mode. Comparison of calculated and observed frequencies in Figure 6 shows a reasonably good fit for the 12D, 11,12-D_2, and 12,14-D_2 derivatives. The ^{13}C shifts are not reproduced accurately, suggesting that the $C_{12}H$ and $C_{14}H$ coordinates should be more strongly mixed in this mode.

[2] In *all-trans*-retinal, the C_9–Me and C_{13}–Me stretches have been assigned at 849 and 866 cm^{-1}, respectively. They shift down in frequency and increase in intensity when the adjacent vinyl protons or the methyl protons are deuteriated (Curry et al., 1982).

[3] The 822-cm^{-1} line in the 12,14,20-D_5 derivative may be the C_{13}–Me stretch which has shifted down and gained intensity. In this case the weak shoulder at 849 cm^{-1} could be due to the $HC_7{=}C_8H$ B_g HOOP mode. Similarly, the 831-cm^{-1} line in 20,14-D_4 bathorhodopsin (Figure 3P) might be the C_{13}–Me stretch.

Table II: Calculated and Observed Hydrogen Out-of-Plane Vibrations (cm^{-1}) for Bathorhodopsin

obsd	calcd	description[a]
		Unmodified Bathorhodopsin
	1006	+0.78 (15H) + 0.38 (NH)
	978	+0.81 (8H) + 0.57 (7H)
	928	+0.96 (NH) − 0.72 (15H) + 0.39 (14H)
921	922	+0.97 (11H) − 0.25 (10H) + 0.23 (12H)
875	874	+0.74 (10H) − 0.70 (7H) + 0.55 (8H)
858	854	+0.88 (12H) + 0.48 (7H) − 0.41 (8H) + 0.40 (10H) + 0.28 (14H)
850	849	+0.90 (14H) − 0.02 (12H) − 0.27 (NH)
838	835	−0.40 (7H) + 0.34 (8H) − 0.64 (10H) + 0.65 (12H)
	809	+0.69 (CH_2) + 0.44 (14H)
		7D Derivative
	932	+1.05 (8H)
	928	+0.96 (NH) − 0.72 (15H) + 0.39 (14H)
920	921	+0.96 (11H)
860	861	+0.93 (10H) + 0.65 (12H)
849	850	+0.90 (14H) + 0.42 (12H)
840	839	+0.81 (12H) − 0.51 (10H) − 0.41 (11H) − 0.35 (14H)
	809	+0.69 (CH2) + 0.44 (14H)
732	734	+0.96 (7D)
		8D Derivative
	928	+0.96 (NH) − 0.72 (15H) + 0.39 (14H)
920	922	+0.97 (11H)
	906	+1.07 (7H)
866	865	+0.98 (10H) + 0.53 (12H)
849	850	+0.87 (14H) + 0.52 (12H)
842	841	+0.84 (12H) − 0.41 (14H) − 0.39 (10H) − 0.43 (11H)
	809	+ 0.69 (CH_2) + 0.44 (14 H)
(765)	760	+ 0.92 (8D)
		10D Derivative
	977	+0.81 (8H) + 0.58 (7H)
	928	+0.96 (NH) − 0.72 (15H) + 0.39 (14H)
919	921	+0.98 (11H)
862	863	+0.97 (7H) − 0.80 (8H)
851	851	+0.87 (12H) + 0.65 (14H)
	846	+0.72 (14H) − 0.69 (12H) − 0.30 (CH2)
827		not assigned
	809	+0.69 (CH2) + 0.44 (14H)
704	706	+0.89 (10D)
		11D Derivative
	978	+0.81 (8H) + 0.57 (7H)
	928	+0.97 (NH) − 0.73 (15H) + 0.40 (14H)
878/870	876	+0.82 (10H) − 0.66 (7H) + 0.52 (8H)
855	854	+0.95 (12H) + 0.42 (7H)
849	849	+0.94 (14H)
	844	+0.65 (10H) − 0.60 (12H) + 0.55 (7H) − 0.47 (8H)
815	810	+0.70 (CH2) + 0.42 (14H)
742	743	+0.87 (11D)
		12D Derivative
	978	+0.81 (8H) + 0.57 (7H)
	928	+0.97 (NH) − 0.73 (15H) + 0.40 (14H)
916	911	+1.07 (11H)
873	873	+0.75 (7H) − 0.60 (8H) − 0.67 (10H)
	849	+0.92 (14H)
841	842	+0.81 (10H) + 0.58 (7H) − 0.49 (8H)
827		not assigned
814	809	+0.69 (CH2) + 0.43 (14H)
699	704	+0.93 (12D)
		14D Derivative
	978	+0.81 (8H) + 0.57 (7H)
	927	+0.94 (NH) − 0.67 (15H) + 0.39 (11H)
916	921	+0.92 (11H)
874	874	+0.74 (10H) − 0.70 (7H) + 0.55 (8H)
849	853	+0.87 (12H) + 0.53 (7H) − 0.45 (8H) + 0.44 (10H) − 0.35 (11H)
	836	+0.68 (10H) − 0.66 (12H) + 0.44 (7H) − 0.37 (8H) + 0.30 (11H)
812	820	+0.77 (CH2)
693	696	+0.88 (14D)
		15D Derivative
	978	+0.81 (8H) + 0.57 (7H)
	949	+1.05 (NH)
923	922	+1.00 (11H)
878	874	+0.74 (10H) − 0.69 (7H) + 0.54 (8H)
862	861	+1.00 (14H) − 0.50 (15D)
854	853	+0.87 (12H) + 0.53 (7H) − 0.45 (8H) + 0.44 (10H) − 0.35 (11H)

Table II (Continued)

obsd	calcd	description[a]
835	836	+0.68 (10H) - 0.66 (12H) + 0.43 (7H) - 0.37 (8H) + 0.31 (11H)
	814	+0.72 (CH2) - 0.38 (15D)
797	796	+0.73 (15D) + 0.45 (14H)
		ND Derivative
	984	+1.06 (15H)
	978	+0.81 (8H) + 0.57 (7H)
921	922	+0.99 (11H)
875	874	+0.75 (10H) - 0.69 (7H) + 0.55 (8H)
859	856	+1.06 (14H) + 0.17 (ND)
851	853	+0.80 (12H) + 0.55 (7H) - 0.47 (8H) + 0.46 (10H) - 0.35 (11H)
	835	+0.66 (10H) - 0.65 (12H) + 0.42 (7H) - 0.35 (8H) + 0.32 (11H)
	830	+0.75 (CH2) + 0.52 (ND)
	733	+0.76 (ND) - 0.23 (14H)

[a] Coefficients ($\delta S/\delta Q$) of hydrogen out-of-plane wags in the normal modes Q. A positive wag coefficient represents hydrogen motion in the $+z$ direction (plane of retinal chromophore is xy plane). Those internal coordinates S contributing more than 10% to the potential energy are listed.

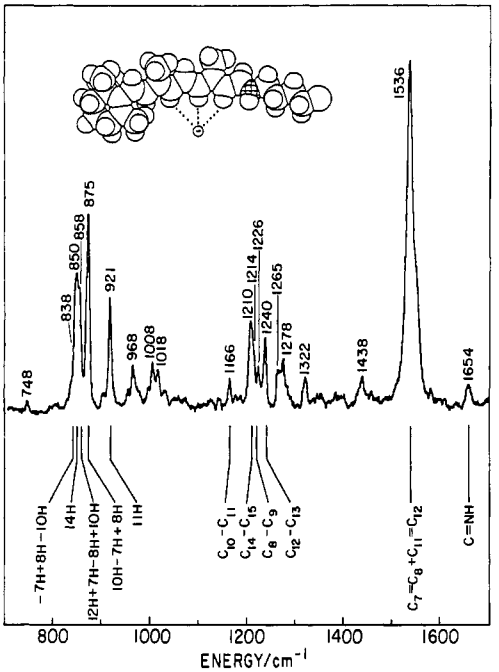

FIGURE 7: Summary of the normal mode assignments for bathorhodopsin. Skeletal stretching assignments are taken from Palings et al. (1987). The inset presents a model for the chromophore in bathorhodopsin that is twisted 20° about the C_8–C_9, C_{10}–C_{11}, C_{12}–C_{13}, and C_{14}–C_{15} bonds and is perturbed by a negatively charged residue near C_{12}.

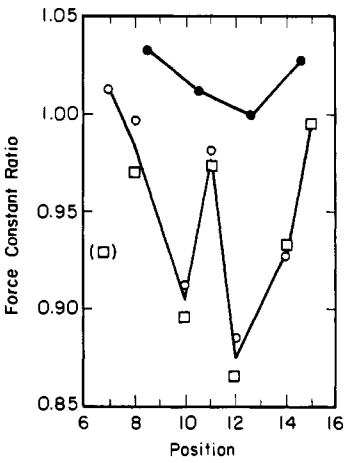

FIGURE 8: Wag force constant ratios for bathorhodopsin/*all-trans*-retinal (○) and for bathorhodopsin/BR_{568} (□). The filled points (●) give the square of the C–C stretch frequency ratios for bathorhodopsin/*all-trans*-retinal protonated Schiff base. The low value for the C_7 wag force constant ratio between bathorhodopsin and BR_{568} is not significant because the chromophores in these pigments have different C_6–C_7 conformations (Harbison et al., 1985; Smith et al., 1987b).

Discussion

Previously, the three lines at 854, 876, and 922 cm^{-1} in bathorhodopsin were assigned to the $C_{14}H$, $C_{10}H$, and $C_{11}H$ wagging vibrations, respectively. The $C_{12}H$ wag was placed in the 860–830-cm^{-1} region, although a specific assignment could not be made (Eyring et al., 1982). The higher resolution spectra and larger set of derivatives reported in this work have allowed us to confirm and extend these assignments. Resolution of the 854-cm^{-1} band into modes at 858, 850, and 838 cm^{-1} followed by a normal mode analysis results in the following assignments: (1) The localized $C_{11}H$ wag is at 921 cm^{-1}. (2) The $C_{10}H$ wag mixed with the $HC_7{=}C_8H$ B_g mode is at 875 cm^{-1}. (3) The $C_{12}H$ wag mixed with the $HC_7{=}C_8H$ B_g and the $C_{10}H$ is at 858 cm^{-1}. (4) The $C_{14}H$ wag is at 850 cm^{-1}. (5) The $HC_7{=}C_8H$ B_g mode mixed with the $C_{10}H$ is at 838 cm^{-1}. The strength of these assignments rests on the shifts observed in individual isotopic derivatives and on the ability of the normal coordinate calculation to consistently describe the mode frequencies in the isotopic derivatives. A large number of assignment schemes and force field iterations were attempted. The field in Table I was the only one that satisfactorily described the modes in the essential isotopic derivatives. These assignments together with previous assignments for the skeletal modes in bathorhodopsin from Palings et al. (1987) are summarized in Figure 7.

On the basis of the normal mode analyses of retinals (Curry et al., 1985), of the *all-trans*-retinal protonated Schiff base (PSB) (Smith et al., 1985), and of BR_{568} (Smith et al., 1987a), we expect the $C_{11}H$ and $C_{12}H$ wags to be strongly coupled in the normal modes while the $C_{10}H$ and $C_{14}H$ wags should be relatively isolated. Bathorhodopsin strongly contrasts with our previous experience: the $C_{11}H$ wag is virtually isolated from the other out-of-plane coordinates including the $C_{12}H$ wag. This uncoupling of the $C_{11}H$ and $C_{12}H$ wag coordinates is partly a consequence of the anomalously low frequency of the $C_{12}H$ mode (858 cm^{-1}) too far away from the $C_{11}H$ wag (921 cm^{-1}) to couple effectively. This qualitative observation is quantitatively supported by the values of the refined out-of-plane force constants. The $C_{12}H$ wag force constant in bathorhodopsin (0.415) is much lower than that for *all-trans*-retinal (0.469), and the 11H × 12H coupling constant is also strongly reduced in bathorhodopsin (0.132) compared to that in retinal (0.168). Comparison of the bathorhodopsin field with that of BR_{568} (Smith et al., 1987a) results in the same conclusion. The coupling constant between adjacent wags is strongly dependent on the π-bond order, changing from ~0.17

for double bonds to ~0.06 for single bonds (Curry et al., 1985). Since the 11H × 12H coupling constant in bathorhodopsin is only 0.132, the C_{11}=C_{12} bond order must be significantly reduced. This presumably contributes to the reduced frequency of the 1536-cm^{-1} ethylenic band compared to rhodopsin and isorhodopsin. Since the individual C=C stretches are highly mixed in the ethylenic normal modes, a quantitative analysis of the ethylenic modes of bathorhodopsin and its isotopic derivatives would be required to fully test this prediction.

Figure 8 presents the wag force constant ratios for bathorhodopsin/*all-trans*-retinal and for bathorhodopsin/BR_{568} plotted versus chain position. The 8H, 11H, and 15H diagonal wag force constants are clearly the least perturbed in bathorhodopsin. The low value of the 7H force constant in bathorhodopsin compared to that in BR_{568} is probably not significant because the chromophore in BR_{568} has a 6-s-trans conformation (Harbison et al., 1985) while bathorhodopsin has a twisted 6-s-cis conformation (Smith et al., 1987b). The C_{10}H, C_{12}H, and C_{14}H wag force constants are significantly lower in bathorhodopsin than they are in BR_{568} and in *all-trans*-retinal, indicating that the vibrational properties at the even-numbered positions in the center of the chain are perturbed.

The filled points in Figure 8 present the ratios squared of the C–C stretch frequencies of bathorhodopsin (Palings et al., 1987) compared to those of the *all-trans*-retinal PSB (Smith et al., 1985). If the normal mode characters are similar, this ratio will be proportional to the effective stretching force constant ratios. A common theme in Figure 8 is the relative depression of the force constant ratios in the center of the chain and especially at C_{12}. This is consistent with the idea proposed earlier by Eyring et al. (1982) and depicted in Figure 7 that a negatively charged protein residue perturbs the bathorhodopsin chromophore near C_{12}. Such a perturbation might account for the reduced C_{10}H, C_{12}H, and C_{14}H wag force constants, the reduced coupling of the C_{11}H with the C_{12}H wags, and the relative reduction of the C_{12}–C_{13} stretch frequency. The reduced coupling between the C_{11}H and C_{12}H wags and the reduced C_{12}–C_{13} stretch frequency are reasonably attributed to polarization of the π-electron structure by the negative charge near C_{12}. The reduced C_{10}H, C_{12}H, and C_{14}H wag force constants may result from distortion of both the σ- and π-bonding at these positions. These perturbations in vibrational properties are the largest that we have seen in retinal proteins. We will next discuss the relation of these observations to the mechanism of energy storage in bathorhodopsin.

A number of mechanisms for the 33 kcal/mol energy storage in bathorhodopsin have been proposed. Honig et al. (1979b) suggested that energy is stored in the form of charge separation caused by isomerization-induced displacement of the positive Schiff base moiety away from its negative counterion. Calculations by Warshel and Barboy (1982) emphasize energy storage through distortion of the chromophore and its immediate protein environment. Hybrid pictures have been presented where conformational distortion of the chromophore and protein accounts for 60% and electrostatic interactions between the counterion and C_{13}···C_{15} accounts for 40% of the stored energy (Birge et al., 1988). The preferred model of Birge et al. (1988) is very similar to that originally proposed by Eyring et al. (1982) which is also strongly supported by this study (see Figure 7).

A large body of experimental data that bears on the mechanism of energy storage has been obtained. Eyring and Mathies (1979) first pointed out that the Schiff base mode in bathorhodopsin is identical to that of rhodopsin. This result has been strongly supported by the studies of Bagley et al. (1985) and Palings et al. (1987). The latter authors emphasized the inconsistency of these Schiff base results with the idea that energy storage arises from translocation of the Schiff base into a new (hydrogen-bonding) environment. This question has recently been examined in more detail by Deng and Callender (1987) and by Rodman Gilson et al. (1988), whose MINDO calculations show that any significant change in hydrogen-bonding environment should alter the Schiff base frequency. Since no significant perturbation of the Schiff base properties of bathorhodopsin is observed, there is little direct experimental support for the Schiff base model of energy storage. On the other hand, large perturbations are observed in the C–C stretch frequencies of bathorhodopsin (Palings et al., 1987) and in the HOOP mode frequencies and intensities (Eyring et al., 1982) compared to the *all-trans*-retinal PSB and to BR_{568} (Figures 7 and 8). The resonance Raman intensities of the HOOP modes have been qualitatively modeled by conformational distortion of the chromophore due to steric interaction with protein residues in the binding site (Eyring et al., 1980a; Warshel & Barboy, 1982). Thus, the hypothesis that energy is stored in bathorhodopsin through conformational distortion of the chromophore has some experimental support. However, the perturbed HOOP mode frequencies and C–C stretch frequencies have never been, even qualitatively, modeled correctly (Eyring et al., 1980a; Warshel & Barboy, 1982; Birge et al., 1988). Since conformational distortions appear to be insufficient to produce these frequency perturbations (Eyring et al., 1980a; Warshel & Barboy, 1982), it is natural to suggest that electrostatic interactions are also important.

The idea that a negatively charged protein residue is an important spectroscopic determinant in bovine rhodopsin was first suggested by Arnaboldi et al. (1979) and by Honig et al. (1979a). Recent solid-state NMR data on ^{13}C-labeled pigments provide additional evidence that there is an electronegative perturbation near C_{13} in rhodopsin (Lugtenburg et al., 1988; Smith et al., 1989). The absence of any perturbation of the C–C stretch frequencies of rhodopsin compared to those of the 11-*cis*-retinal PSB does not support nor does it necessarily rule out the presence of such a charge (Palings et al., 1987). The sensitivity of the C–C mode frequencies to such a charge perturbation may be weak as suggested by the calculations of Birge et al. (1988). It should be noted, however, that isorhodopsin does exhibit significant C–C stretch frequency shifts compared to the 9-cis PSB in solution (Palings et al., 1987). Thus, there is now a wide base of support for the presence of a charged residue in the binding pocket which could perturb the chromophore in bathorhodopsin. Now that the perturbations of the skeletal C–C stretching modes and of the HOOP modes in bathorhodopsin have been clearly identified, it should be possible to model the binding site interactions with theoretical calculations to determine whether such a charge perturbation can help to account for the unique vibrational properties of bathorhodopsin and the 33 kcal/mol energy storage.

Acknowledgments

We thank Albert Broek and Hans Pardoen for expert assistance in the synthesis of the retinal isotopic derivatives, Tom Pollard for writing the Lorentzian band deconvolution program and Bo Curry for assistance with the normal mode calculations.

Supplementary Material Available

An unabbreviated summary of the experimental and theoretical out-of-plane frequencies and normal modes (Table III)

and the Cartesian coordinates used in the calculation (Table IV) (5 pages). Ordering information is given on any current masthead page.

References

Applebury, M. L., Zuckerman, D. M., Lamola, A. A., & Jovin, T. M. (1974) *Biochemistry 13*, 3448.

Arnaboldi, M., Motto, M. G., Tsujimoto, K., Balogh-Nair, V., & Nakanishi, K. (1979) *J. Am. Chem. Soc. 101*, 7082.

Aton, B., Doukas, A. G., Narva, D., Callender, R. H., Dinur, U., & Honig, B. (1980) *Biophys. J. 29*, 79.

Bagley, K. A., Balogh-Nair, V., Croteau, A. A., Dollinger, G., Ebrey, T. G., Eisenstein, L., Hong, M. K., Nakanishi, K., & Vittitow, J. (1985) *Biochemistry 24*, 6055.

Birge, R. R. (1981) *Annu. Rev. Biophys. Bioeng. 10*, 315.

Birge, R. R., & Hubbard, L. M. (1980) *J. Am. Chem. Soc. 102*, 2195.

Birge, R. R., & Hubbard, L. M. (1981) *Biophys. J. 34*, 517.

Birge, R. R., Einterz, C. M., Knapp, H. M., & Murray, L. P. (1988) *Biophys. J. 53*, 367.

Braiman, M., & Mathies, R. (1982) *Proc. Natl. Acad. Sci. U.S.A. 79*, 403.

Broek, A. D., & Lugtenburg, J. (1980) *Recl. Trav. Chim. Pays-Bas 99*, 363.

Broek, A. D., & Lugtenburg, J. (1982) *Recl. Trav. Chim. Pays-Bas 101*, 102.

Cooper, A. (1979) *Nature (London) 282*, 531.

Courtin, J. M. L., 't Lam, G. K., Peters, A. J. M., & Lugtenburg, J. (1985) *Recl. Trav. Chim. Pays-Bas 104*, 281.

Curry, B. U. (1983) Ph.D. Thesis, University of California, Berkeley, CA 94720.

Curry, B., Broek, A., Lugtenburg, J., & Mathies, R. (1982) *J. Am. Chem. Soc. 104*, 5274.

Curry, B., Palings, I., Broek, A., Pardoen, J. A., Mulder, P. P. J., Lugtenburg, J., & Mathies, R. (1984) *J. Phys. Chem. 88*, 688.

Curry, B., Palings, I., Broek, A. D., Pardoen, J. A., Lugtenburg, J., & Mathies, R. (1985) *Adv. Infrared Raman Spectrosc. 12*, 115.

Deng, H., & Callender, R. H. (1987) *Biochemistry, 26*, 7418.

Eyring, G., & Mathies, R. (1979) *Proc. Natl. Acad. Sci. U.S.A. 76*, 33.

Eyring, G., Curry, B., Mathies, R., Fransen, R., Palings, I., & Lugtenburg, J. (1980a) *Biochemistry 19*, 2410.

Eyring, G., Curry, B., Mathies, R., Broek, A., & Lugtenburg, J. (1980b) *J. Am. Chem. Soc. 102*, 5390.

Eyring, G., Curry, B., Broek, A., Lugtenburg, J., & Mathies, R. (1982) *Biochemistry 21*, 384.

Fransen, M. R., Palings, I., Lugtenburg, J., Jansen, P. A. A., & Groenendijk, G. W. T. (1980) *Recl. Trav. Chim. Pays-Bas 99*, 384.

Harbison, G. S., Smith, S. O., Pardoen, J. A., Courtin, J. M. L., Lugtenburg, J., Herzfeld, J., Mathies, R. A., & Griffin, R. G. (1985) *Biochemistry 24*, 6955.

Honig, B., Dinur, U., Nakanishi, K., Balogh-Nair, V., Gawinowicz, M. A., Arnaboldi, M., & Motto, M. G. (1979a) *J. Am. Chem. Soc. 101*, 7084.

Honig, B., Ebrey, T., Callender, R. H., Dinur, U., & Ottolenghi, M. (1979b) *Proc. Natl. Acad. Sci. U.S.A. 76*, 2503.

Loppnow, G. R., & Mathies, R. A. (1988) *Biophys. J. 54*, 35.

Lugtenburg, J. (1984) in *Spectroscopy of Biological Molecules*, NATO ASI Series C, Vol. 139, pp 447–455, Reidel, Dordrecht.

Lugtenburg, J. (1985) *Pure Appl. Chem. 57*, 753.

Lugtenburg, J., Mathies, R. A., Griffin, R. G., & Herzfeld, J. (1988) *Trends Biochem. Sci. 13*, 388.

Oseroff, A. R., & Callender, R. H. (1974) *Biochemistry 13*, 4243.

Palings, I. (1987) Ph.D. Thesis, University of California, Berkeley, CA 94720.

Palings, I., Pardoen, J. A., van den Berg, E., Winkel, C., Lugtenburg, J., & Mathies, R. A. (1987) *Biochemistry 26*, 2544.

Pardoen, J. A., Neijenesch, H. N., Mulder, P. P. J., & Lugtenburg, J. (1983) *Recl. Trav. Chim. Pays-Bas 102*, 341.

Pardoen, J. A., Winkel, C., Mulder, P. P. J., & Lugtenburg, J. (1984) *Recl. Trav. Chim. Pays-Bas 103*, 135.

Pardoen, J. A., Mulder, P. P. J., van den Berg, E. M. M., & Lugtenburg, J. (1985) *Can. J. Chem. 63*, 1431.

Pardoen, J. A., van den Berg, E. M. M., Winkel, C., & Lugtenburg, J. (1986) *Recl. Trav. Chim. Pays-Bas 105*, 92.

Peters, K., Applebury, M. L., & Rentzepis, P. M. (1977) *Proc. Natl. Acad. Sci. U.S.A. 74*, 3119.

Rodman Gilson, H. S., Honig, B. H., Croteau, A., Zarrilli, G., & Nakanishi, K. (1988) *Biophys. J. 53*, 261.

Schick, G. A., Cooper, T. M., Holloway, R. A., Murray, L. P., & Birge, R. R. (1987) *Biochemistry 26*, 2556.

Smith, S. O., Myers, A. B., Mathies, R. A., Pardoen, J. A., Winkel, C., van den Berg, E. M. M., & Lugtenburg, J. (1985) *Biophys. J. 47*, 653.

Smith, S. O., Braiman, M. S., Myers, A. B., Pardoen, J. A., Courtin, J. M. L., Winkel, C., Lugtenburg, J., & Mathies, R. A. (1987a) *J. Am. Chem. Soc. 109*, 3108.

Smith, S. O., Palings, I., Copie, V., Raleigh, D. P., Courtin, J., Pardoen, J. A., Lugtenburg, J., Mathies, R. A., & Griffin, R. G. (1987b) *Biochemistry 26*, 1606.

Smith, S. O., Palings, I., Miley, M. E., Courtin, J. M. L., de Groot, H. J. M., Lugtenburg, J., Mathies, R. A., & Griffin, R. G. (1989) *Biochemistry* (in preparation).

Warshel, A., & Barboy, N. (1982) *J. Am. Chem. Soc. 104*, 1469.

Wilson, E. B., Decius, J. C., & Cross, P. C. (1955) *Molecular Vibrations*, McGraw-Hill, New York.

Yoshizawa, T., & Wald, G. (1963) *Nature (London) 197*, 1279.